

# Lawrence Berkeley National Laboratory

## Recent Work

### Title

A SEGMENTED POSITION-SENSITIVE PLASTIC PHOSWICH DETECTOR

### Permalink

<https://escholarship.org/uc/item/37c488s4>

### Author

Schmidt, H.R.

### Publication Date

1985-07-01



# Lawrence Berkeley Laboratory

UNIVERSITY OF CALIFORNIA

RECEIVED  
LAWRENCE  
BERKELEY LABORATORY

JUL 2 1985

LIBRARY AND  
DOCUMENTS SECTION

Submitted to Nuclear Instruments and Methods

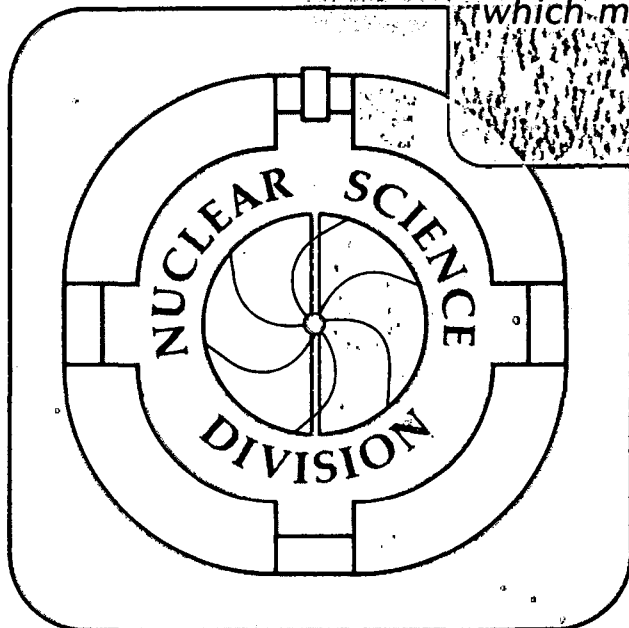
A SEGMENTED POSITION-SENSITIVE PLASTIC  
PHOSWICH DETECTOR

H.R. Schmidt, M. Bantel, Y. Chan, S.B. Gazes,  
S. Wald, and R.G. Stokstad

July 1985

TWO-WEEK LOAN COPY

*This is a Library Circulating Copy  
which may be borrowed for two weeks.*



LBL-19910  
2

## **DISCLAIMER**

This document was prepared as an account of work sponsored by the United States Government. While this document is believed to contain correct information, neither the United States Government nor any agency thereof, nor the Regents of the University of California, nor any of their employees, makes any warranty, express or implied, or assumes any legal responsibility for the accuracy, completeness, or usefulness of any information, apparatus, product, or process disclosed, or represents that its use would not infringe privately owned rights. Reference herein to any specific commercial product, process, or service by its trade name, trademark, manufacturer, or otherwise, does not necessarily constitute or imply its endorsement, recommendation, or favoring by the United States Government or any agency thereof, or the Regents of the University of California. The views and opinions of authors expressed herein do not necessarily state or reflect those of the United States Government or any agency thereof or the Regents of the University of California.

# A SEGMENTED POSITION-SENSITIVE PLASTIC PHOSWICH DETECTOR

H.R. Schmidt, M. Bantel<sup>a)</sup>, Y. Chan, S.B. Gazes,  
S. Wald<sup>b)</sup> and R.G. Stokstad

**Nuclear Science Division, Lawrence Berkeley Laboratory,  
University of California, Berkeley, CA 94720**

**a) Now at Max-Planck-Institut für Kernphysik, Germany**

**b) Now at Weizmann Institute of Science, Israel**

For the detection of light particles we have built a multi-element detector, consisting of eight position-sensitive strips. The total active area is  $20 \times 20 \text{ cm}^2$ . The strips are of the phoswich type, having a thin element of fast NE102 (decay time  $\tau=2.5 \text{ ns}$ ) and a thick element of slow NE115 ( $\tau=225 \text{ ns}$ ). The position information is obtained by making use of light attenuation through surface losses. The detector is able to identify protons, deuterons and  $\alpha$  particles. The position and energy resolutions were found to vary from 4 to 18 mm (FWHM) and 2.2 to 5.8 % (FWHM), respectively, for  $\alpha$  energies ranging from 87 to 35 MeV. The detector has been used in experiments for the coincident measurement of light particles produced in heavy-ion-induced reactions.

# I INTRODUCTION

The mechanisms for heavy-ion reactions become increasingly complicated at higher bombarding energies. Coincidence measurements are required in order to trace the many possible reaction pathways. As has been reported recently, [1] the topology of experimental correlations can be affected both by the reaction mechanisms as well as the phase-space limitations imposed by the finite solid angle of the detector. To minimize these phase-space limitations, large-area detectors are desired.

Such a detector has been described recently [2]. This detector has an active area of  $20 \times 20 \text{ cm}^2$  and makes use of the "phoswich" technique [3,4] to identify light particles. The interesting features of the detector are the use of plastic scintillator material for both the  $\Delta E$  and  $E$  elements of the phoswich, and the two-dimensional continuous position sensitivity derived from light loss arising naturally from multiple internal reflections of a non-ideal scintillator surface [5]. The phoswich detector of Ref. 2 does not provide multiple-hit information, since the active area consists of a single  $20 \times 20 \text{ cm}^2$  phoswich sheet. In this article, we report on the performance of a detector which is similar to the above one, but allows multiple-hit detection. To achieve this, we gave up continuous position information in one direction by segmenting the detector plane into eight separate strips (Fig. 1), whereby each strip has one phototube at each end. We kept the total size of the detector at  $20 \times 20 \text{ cm}^2$  to allow the replacement of individual elements of the  $4\pi$ -Plastic Box detector [6]. Section II describes the design of the segmented phoswich detector. Since the previous article by M. Bantel et al. [2] contains most of the design details of a plastic phoswich detector, we concentrate here on the new features. In Sec. III, we discuss the corrections which have to be applied to the raw data in order to obtain the energy and position of the particles. In Sec. IV, we describe the performance of this detector in actual experiments.

## II DESIGN

To achieve  $\Delta E$ -E particle identification, we employed the phoswich technique of coupling a fast and a slow scintillator together. While most other phoswiches reported in the literature use a thin slice of  $\text{CaF}_2$  as the first  $\Delta E$  element, in our case both the  $\Delta E$  and the E counter are made of plastic. The first element is made of the familiar plastic scintillator NE102, which has a fast decay time constant of 2.5 ns. For the E element, we took the new plastic material NE115, which has a relatively long decay time of 225 ns. The use of a fast scintillator for the  $\Delta E$  element has the advantage that one gains good timing even for particles which are stopped in the first layer of the phoswich. Furthermore, due to the higher light output of NE102 compared to NE115, a reduction in thickness for the  $\Delta E$  element is possible. The properties of the new scintillator are described in Ref. 2.

The whole detector consists of eight individual strips. Each strip is  $20 \times 2.5 \text{ cm}^2$  in area. The  $\Delta E$  and E layer are 0.5 and 4.5 mm thick, respectively. The two layers are glued together only at the very ends of a strip (see Fig. 2) to avoid a dead layer of optical cement over the entire strip. Therefore, the  $\Delta E$  and E layer are optically decoupled along the strip and the attenuation of the light produced in the first layer depends sensitively on its thickness. The features of this form of light attenuation in a thin scintillator are described in Ref. 2. Protons up to 20 MeV and  $\alpha$  particles up to 90 MeV can be stopped. The  $\Delta E$  layer stops protons with  $E < 6 \text{ MeV}$  and  $\alpha$  particles with  $E < 22 \text{ MeV}$ . In principle, the  $\Delta E$ -E particle identification could be extended to lower energies by reducing the thickness of the  $\Delta E$  layer. In practice, however, light produced in a thinner  $\Delta E$  sheet is attenuated so much as the light travels along the strip to the phototubes that one has severe signal-to-noise problems. Fig. 2 shows a top (A) and a side (B) view of one element of the detector. Note that the scales of (A) and (B) are different. Fig. 2A shows the shape and the dimensions of a strip and the area where the phototubes are attached to the strip. As can be seen from Fig. 2B, the tubes are glued directly onto the scintillator without using a light guide. The edges at the ends of the strip are beveled at  $45^\circ$ , polished, and aluminized. Each edge acts as a  $90^\circ$  mirror that reflects the light into the phototube. The light is detected with 3/4-inch Hamamatsu R1450 phototubes equipped with E974-05 Hamamatsu bases.

### III ENERGY AND POSITION DETERMINATION

A typical signal from the phoswich has a fast rising spike from the NE102 plastic and a slow decaying tail from the NE115 backing. The signal is analyzed by two independent charge-sensitive CAMAC ADS's with short ( $t_0$  to  $t_s$ ) and long ( $t_0$  to  $t_l$ ) integrating gate width settings. Therefore, a single event in one strip is defined by four parameters:  $\Delta I_T$  and  $\Delta I_B$  resulting from the short gates applied to the signals from the top and bottom phototubes, and  $I_T$  and  $I_B$  from the long gate. The signals have a strong dependence on the position of the incident particle hitting the strip. This behavior is shown in Fig. 3. The data points correspond to 87-MeV  $\alpha$  particles hitting at various positions along a strip. The measured light output at one end of the scintillator is then plotted as a function of position. The solid line is the result of a Monte-Carlo calculation which assumes light attenuation through surface losses (see Ref. 2). The position dependence of the PMT signals  $I_T$ ,  $I_B$ ,  $\Delta I_T$  and  $\Delta I_B$  is found to be described empirically by the following equations:

$$I_T = \epsilon \cdot N \cdot \exp(+ax + bx^2), \quad (1a)$$

$$I_B = \epsilon \cdot N \cdot \exp(-ax + bx^2), \quad (1b)$$

$$\Delta I_T = \epsilon' \cdot \Delta N \cdot \exp(+a'x + b'x^2), \quad (1c)$$

$$\Delta I_B = \epsilon' \cdot \Delta N \cdot \exp(-a'x + b'x^2), \quad (1d)$$

where  $\epsilon$ ,  $\epsilon'$  are the normalization factors,  $N$  and  $\Delta N$  the number of light quanta that fall within the long and the short gate, respectively, and  $x$  is the position on the strip. The coefficients  $a, a', b$  and  $b'$  depend on the material and geometry of the strip and, in general, have to be determined by a position calibration.  $N$  is the sum of light quanta produced in the fast and the slow scintillators:

$$N = N_f + N_s. \quad (2)$$

The number  $\Delta N$  contains a portion of photons from the thick plastic (NE115) that are accepted in the short gate:

$$\Delta N = N_f + \Delta N_s \quad (3)$$

The correction  $\Delta N_s$  can be calculated from the known decay constant  $\tau$  of NE115 and the durations of  $t_s$  and  $t_l$ , the short and long gates, respectively. The component of light from the slow scintillator contained in  $\Delta N$  is given by

$$\Delta N_s = (N - \Delta N) \frac{\int_0^{t_s} \exp(-t/\tau) dt}{\int_0^{t_l} \exp(-t/\tau) dt} \quad (4)$$

A multiplication of the top and bottom signals,  $I_B \cdot I_T$ , removes the linear term in the argument of the exponential function and yields  $N$  and  $\Delta N$ :

$$N = \epsilon \cdot \sqrt{I_T \cdot I_B} / \exp(bx^2), \quad (5a)$$

$$\Delta N = \epsilon' \cdot \sqrt{\Delta I_T \cdot \Delta I_B} / \exp(b'x^2). \quad (5b)$$

The coefficients  $b$  and  $b'$  have to be determined by a position calibration and were found to be  $b \approx b' \approx 0.0042 \text{ cm}^{-2}$ . The position  $x$  can be calculated from

$$x = (2a)^{-1} \cdot \ln(I_T / I_B), \quad (6)$$

where  $a \approx 0.11 \text{ cm}^{-1}$  also comes from a position calibration. A simple formula connecting the light output  $N$  with the energy of the incident particle is [7]

$$N = P(Z, A)^{-0.63} \cdot E^Y, \quad (7)$$

where  $P(A, Z)^{-0.63}$  is a factor dependent on the type of particle. The total energy  $E$  as well as the energy loss  $\Delta E$  in the thin plastic can be calculated from the measured quantities  $I_T$ ,  $I_B$ ,  $\Delta I_T$  and  $\Delta I_B$ , using the above equations (2)-(6) and inverting (8a) and (8b).

$$N_f = P(Z, A)^{-0.63} \cdot [E^Y - (E - \Delta E)^Y], \quad (8a)$$

$$N_s = r \cdot P(Z, A)^{-0.63} \cdot (E - \Delta E)^Y. \quad (8b)$$



The quantity  $r$  is the ratio of light output of NE115 and NE102 and was determined to be 0.62 [2]. The exponent  $y$  is fixed by an energy calibration to be  $y=1.26$ .

## IV PERFORMANCE

### IV.1 TEST MEASUREMENTS

The Phoswich strips have been tested using an 87-MeV  $\alpha$  beam from the LBL 88-inch Cyclotron. The beam current was reduced sufficiently so that the direct beam could be used to bombard the strips. Moving the horizontally positioned strip through the beam determined the position response. For each position the 87-MeV  $\alpha$  beam was degraded in energy with aluminum foils of different thickness, providing additional energies of 79, 70, 60, 49, 35.5 and 14.5 MeV. Fig. 4 shows the spectrum of these energies measured with a strip. The figure does not yield the intrinsic energy resolution of the the phoswich detector directly since, for all but the highest energy, the energy spread in the degrader foils has to be taken into account. After correction for energy straggling in the degrader foils [8], the energy resolution was determined to be 2.2, 2.4, 2.7, 3.1, 3.7, 5.8 and 32.8 % (FWHM) for the various energies. The lowest energy  $\alpha$  particles (14.5 MeV) are stopped in the thin  $\Delta E$  layer, which results in a poorer resolution due to the stronger light attenuation in the layer. As shown in Fig. 5, the position resolution is independent of position.

The position was reconstructed according to equation (6). The position resolution is energy dependent and - after correction for beam spread due to multiple scattering in the degrader foils - is 0.4, 0.6, 0.8, 1.0, 1.3, 1.6 and 4.2 cm for  $\alpha$  energies from 87 to 14.5 MeV.

Another test was performed by scattering  $\alpha$  particles from a carbon target. The middle of the strip was located at  $43^\circ$  at a distance of 25 cm from the target. The result of this test is illustrated by a plot of the energy loss in the first layer versus the total energy deposited in the scintillators (Fig. 6). Two bands are clearly defined and represent  $\alpha$  particles and hydrogen isotopes. The lower band contains mainly protons, but it shows also a separated group of deuterons and tritons. A projection of  $\alpha$  particles on the

energy axis is given in Fig. 7. It shows the resolution of the ground and first excited states of the  $^{12}\text{C}$  target. Given the thickness of the  $\Delta E$  layer, the spectrum is cut at about 22 MeV for  $\alpha$ 's. The good timing properties of plastic scintillator, however, should enable the separation of  $\alpha$ 's and protons stopped in the first layer from other particles by time of flight.

Finally, the (relative) detection efficiency, especially near the edges, was measured by irradiating the strip with scattered  $\alpha$  particles which passed through a thin, tightly-collimated silicon counter. The efficiency was obtained by comparing the number of  $\alpha$  particles registered by the silicon detector to the number of particles detected by the phoswich strip in coincidence. The efficiency is 100% across the strip except at the edges where it drops rapidly to zero. The absence of strong edge-effects allows the strips to be used without collimating masks.

## IV.2 EXPERIMENTS

The detector was used in an experiment in which a  $^{197}\text{Au}$  target was bombarded with an 11-MeV/A  $^{20}\text{Ne}$  beam from the LBL 88-Inch Cyclotron. The purpose of this experiment was to measure energy and angular correlations of heavy projectile-like fragments and fast, forward-peaked light fragments. The experimental setup consisted of a  $\Delta E$ -E silicon telescope at  $28^\circ$ , directly in front of the center of the phoswich detector. Fig. 8 shows an image of the positions of the  $\alpha$  particles hitting the phoswich detector in coincidence with beam-velocity  $^{16}\text{O}$  ejectiles. Since the plastic detector is position-sensitive only along its strips (the y-direction), data are randomized across the individual segments (the x-direction). These randomized positions are used for all further calculations, where position information in x is required. It automatically takes into account the error propagation due to the uncertainty in position because of discrete position sensitivity in the x-direction. The figure shows a cone of  $\alpha$  particles accompanying the  $^{16}\text{O}$  ions. The dip in the center of the figure results from both the partial shadowing of the strips by the trigger telescope as well as from the sequential-breakup kinematics of the excited  $^{20}\text{Ne}$  primary fragments.

Fig. 9a shows a two-dimensional plot of oxygen energy versus  $\alpha$ -particle energy. The plot shows a groundstate-groundstate band together with some unresolved excited states. Under the assumption that  $\alpha$ - $^{16}\text{O}$  coincidences are produced by sequential decay of  $^{20}\text{Ne}$  [9], the distribution of excitation energy in the primary  $^{20}\text{Ne}$  above the  $\alpha$  threshold can be reconstructed from

the momenta of the two fragments. This is illustrated in Fig. 9b.

The most forward strips were operated at count rates of about 40 kHz, due mostly to elastic scattering of the  $^{20}\text{Ne}$ -beam. We observed a saturation effect of the phototubes at about 80 kHz. Since in experiments of this kind the limiting factor is usually the counting rate of the phoswich detector, the segmentation of the single-element  $20 \times 20 \text{ cm}^2$  phoswich of Ref. 2 into eight electronically independent strips permits for operation at higher beam currents, hence improving the overall efficiency of data accumulation.

Another problem we encountered was that, in order to guarantee a reasonable dynamic range for particles hitting the middle section of a strip, a relatively high photomultiplier tube voltage was applied. This, however, produces an overflow in the charge to digital converters (QDC's) for particles hitting the strip close to an end. This is partly due to the 256 pC range of the LeCroy 2249A QDC's we used, but mainly due to the strong exponential dependence of the light output upon the position. To have a full dynamic range over the entire detector, it would be wise to use a thicker E plastic, resulting in less attenuation. Even though one would intuitively expect that a thicker plastic would degrade the position resolution, a simple estimate shows that the statistical error on  $x$  (eq. 6) due to a weaker position dependence of the two signals increases only near the very ends of the strip. However, one can afford this because the statistical error on  $x$  near the ends is reduced because the light collection efficiency is large.

One of the design goals of the segmented phoswich has been the capability to record multiple hits; in other words, to measure three-fold and higher coincidences. The reaction  $^{197}\text{Au}(^{20}\text{Ne}, ^{12}\text{C}\alpha\alpha)$  has been used to test this feature. Fig. 10a shows the  $\alpha\alpha$ -rate as a function of the angle between the two  $\alpha$  particles hitting the slice detector in coincidence with a  $^{12}\text{C}$  particle measured in the silicon detector. The information about the opening angle, as well as the energies of the two  $\alpha$  particles, can be used in attempting to reconstruct the reaction pathway leading to this particular final state; e.g., to decide whether an intermediate  $^8\text{Be}$  nucleus is formed by the decay of  $^{20}\text{Ne}$ . The angular resolution is, of course, limited by the finite size of the individual strips. Furthermore, there is a certain probability  $P_{\alpha\alpha}$  that the two  $\alpha$  particles will hit the same strip. This probability  $P_{\alpha\alpha}$  as a function of angle  $\xi_{\alpha\alpha}$  between the two  $\alpha$  particles has been evaluated by means of a Monte-Carlo calculation and is shown in Fig. 10b. Fig. 10a has not been folded with this correction.

## V SUMMARY

A plastic scintillator detector consisting of eight elements, each 20 x 2.5 cm<sup>2</sup>, has been constructed and used to detect light particles in coincidence with heavy ions. Particle identification is achieved through a  $\Delta E$ -E phoswich design and position information along a given strip through observation of the light collected at each end. The energy and position resolution were sufficient to observe and study the sequential decay of excited projectile-like fragments produced in the  $^{20}\text{Ne} + ^{197}\text{Au}$  reaction. The capability of the system to detect more than one particle at a time was used to observe two  $\alpha$  particles in coincidence with  $^{12}\text{C}$  ions.

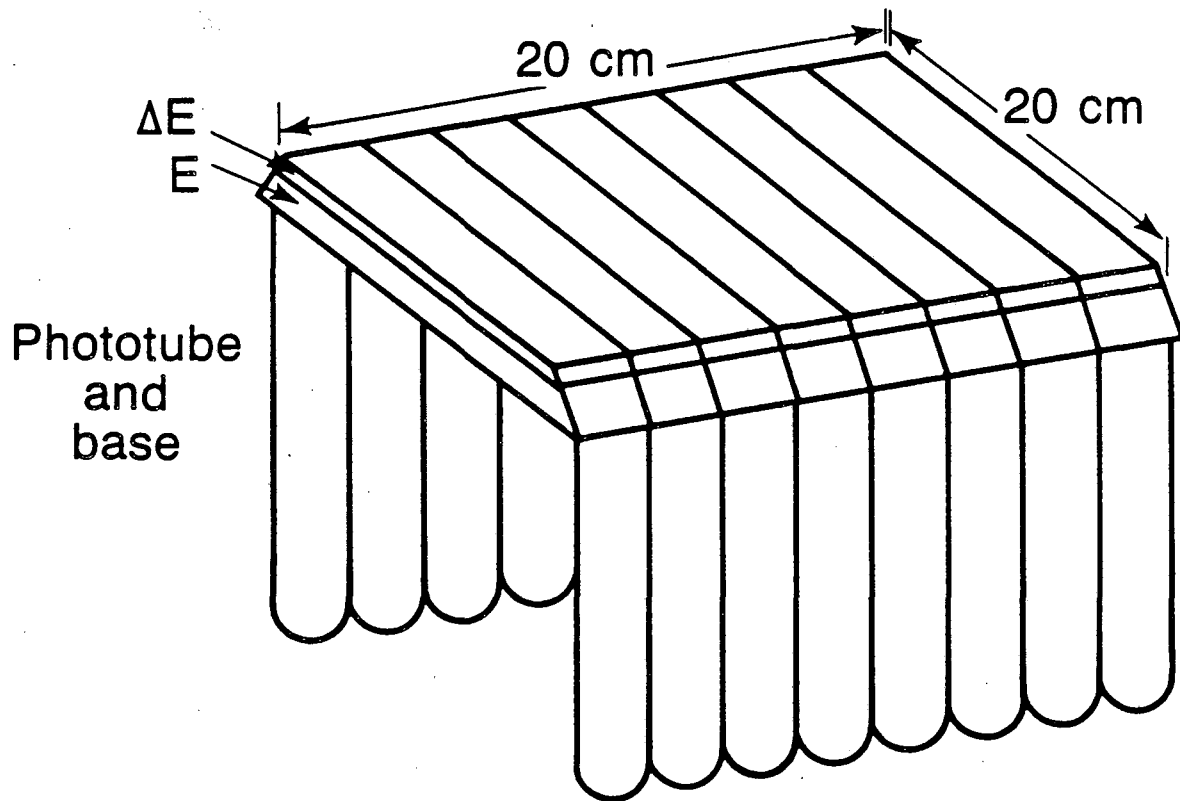
This work was supported by the Director, U.S. Office of Energy Research, Division of Nuclear Physics of the Office of High Energy Nuclear Physics, and by the Nuclear Sciences of Basic Energy Sciences Program of the U.S. Department of of Basic Energy Sciences Program of the U.S. Department of Energy under contract Nos. DE-AC03-76SF00098 and DE-AM03-76SF00326.

## REFERENCES

1. M.J. Murphy, S. Gil, M.N. Harakeh, A. Ray, A.G. Seamster, R. Vandenbosch and T.C. Awes, Phys. Rev. Lett. 53 (1984) 1543
2. M. Bantel, R.G. Stokstad, Y.D. Chan, S. Wald and P.J. Countryman, Nucl. Instr. and Meth. 226 (1984) 394
3. A. Baden, H.H. Gutbrod, H. Lohner, M.R. Maier, A.M. Poskanzer, T. Renner, H. Riedesel, H.G. Ritter, H. Spieler, A. Warwick, F. Weik and H. Wieman, Nucl. Instr. and Meth. 203 (1982) 189.
4. C. Pastor, F. Benrachi, B. Chambon, D. Drain, A. Dauchy, A. Giorni and C. Morand, Nucl. Instr. and Meth. 212 (1983) 209.
5. J.F. Arens, Nucl. Instr. and Meth. 120 (1974) 275.  
J.V. Geaga, G.J. Igo, J.B. McClelland, M.A. Nasser, S. Sander, H. Spinka, D.A. Treadway, J.B. Carroll, D. Fredrickson, V. Perez-Mendez, E.T.B. Whipple, Nucl. Instr. and Meth. 141 (1977) 263
6. K. Van Bibber, et al., IEEE Trans. Nucl. Sci. NS-31 35 (1984).  
R.G. Stokstad, et al., Proceedings of the International Symposium on Heavy-Ion Physics, Mt Fuji, Japan, (1984). To be published by the Physical Society of Japan.  
S. Wald et al., to be published in Phys. Rev. C.
7. F.D. Bechetti, C.E. Thorn and M.J. Levine, Nucl. Instr. and Meth. 138 (1976) 93
8. J.B. Marion and B.A. Zimmerman, Nucl. Instr. and Meth. 51 (1967) 93.
9. H. Homeyer, M. Burgel, M. Clover, Ch. Egelhaaf, H. Fuchs, A. Gamp, D. Kovar and W. Rauch, Phys. Rev. C26 (1982) 1335

## FIGURE CAPTIONS

1. A sketch of the segmented phoswich detector.
2. Details of the phoswich detector. (A) shows a top view of one of the strips. The hatched area shows where the phototubes are mounted. (B) shows, on a larger scale, a side view of one of the ends of a strip.
3. The light collected at one end of a thin strip 20 cm long and 2.5 cm wide. Results are given as a function of incident beam position along the strip. The solid line shows results of a Monte-Carlo calculation described in Ref. 2.
4. Energy spectra for  $\alpha$  particles of different energies. The various  $\alpha$  energies were generated with the help of aluminum degrader foils of different thickness. The number of counts in each peak is arbitrary.
5. Position spectrum of an 87-MeV  $\alpha$  beam hitting a strip at different positions. The number of counts in each peak is arbitrary.
6.  $\Delta E$ -versus- $E_{\text{total}}$  plot of the reaction of 87-MeV  $\alpha$  particles with  $^{12}\text{C}$ . The plot is generated by gating on a narrow region of the position spectrum of one strip of the phoswich detector.
7. Projection of the  $\alpha$  particles of Fig. 6 on the energy axis.
8. A scatterplot of the xy-coordinates of  $\alpha$  particles in coincidence with  $^{16}\text{O}$  ions at the center of the detector. For details see text.
9. (A): Plot of  $^{16}\text{O}$  energy vs.  $\alpha$  energy. (B): Reconstruction of the excitation energy of the primary  $^{20}\text{Ne}$  under the assumption of a sequential-breakup mechanism.
10. (A): Spectrum of the opening angles of two  $\alpha$  particles hitting the detector in coincidence with  $^{12}\text{C}$ . (B): Monte-Carlo estimate of the percentage of two  $\alpha$  particles hitting the same slice as a function of opening angle.



XBL 8411-6343

Fig. 1

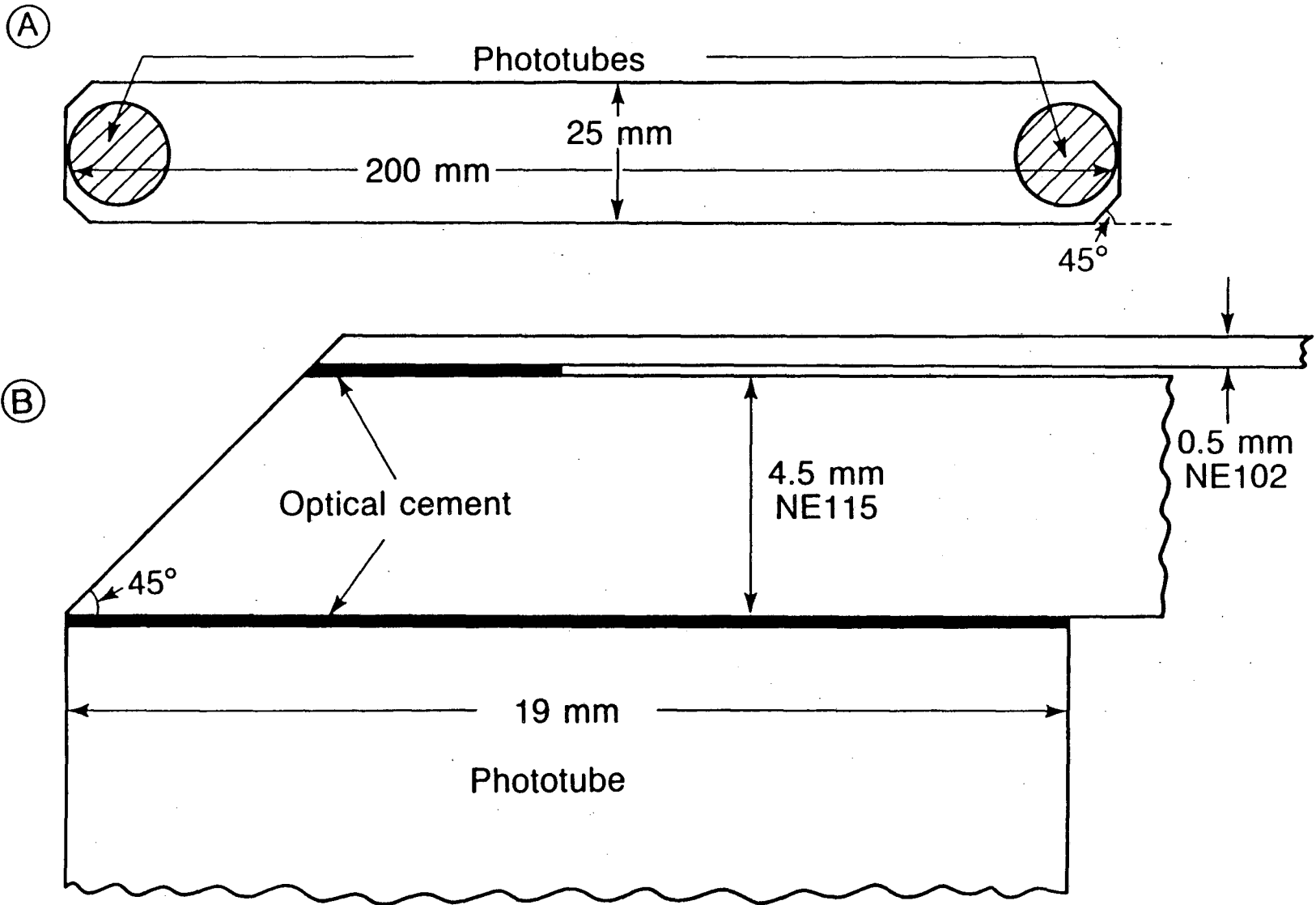
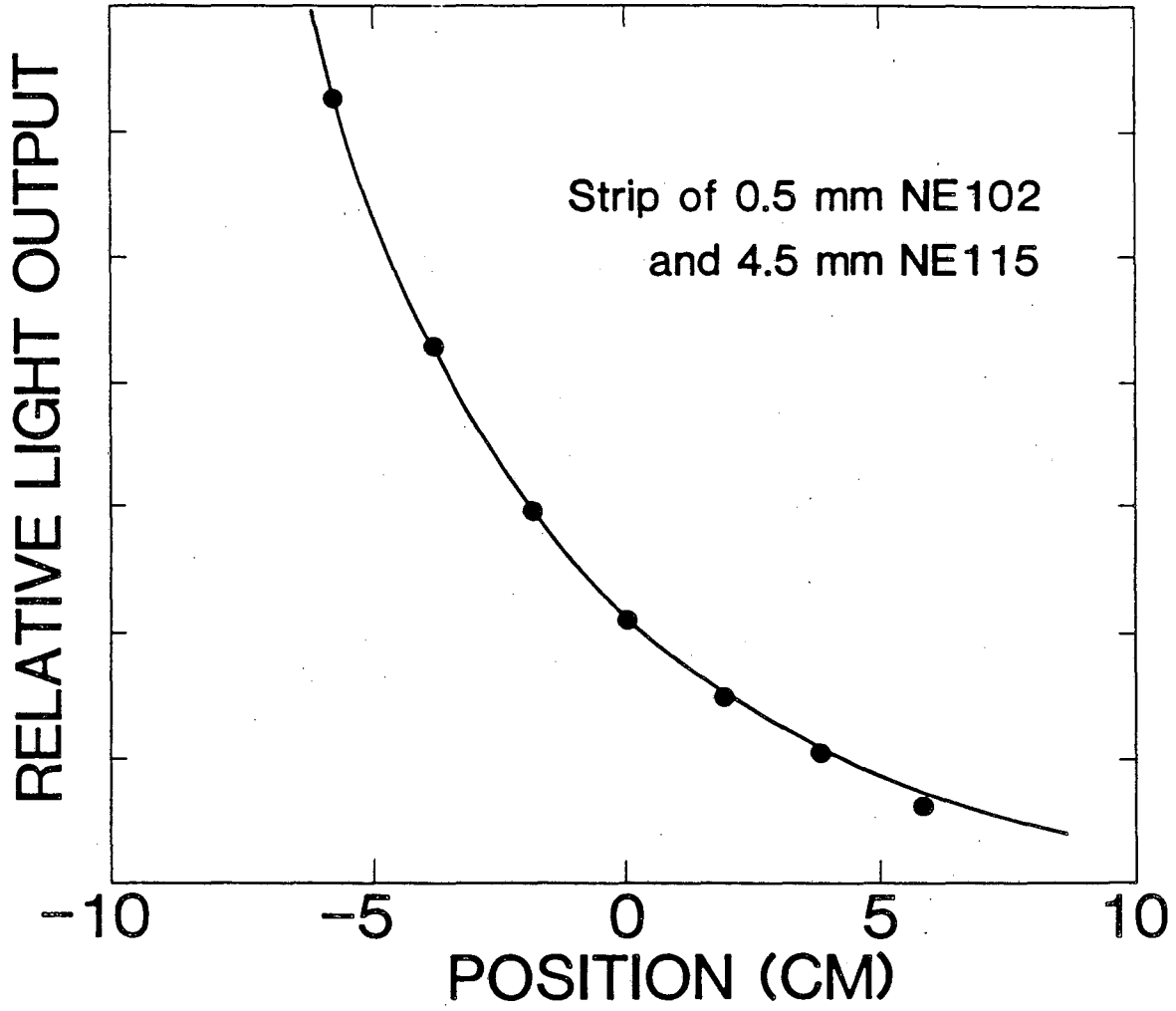


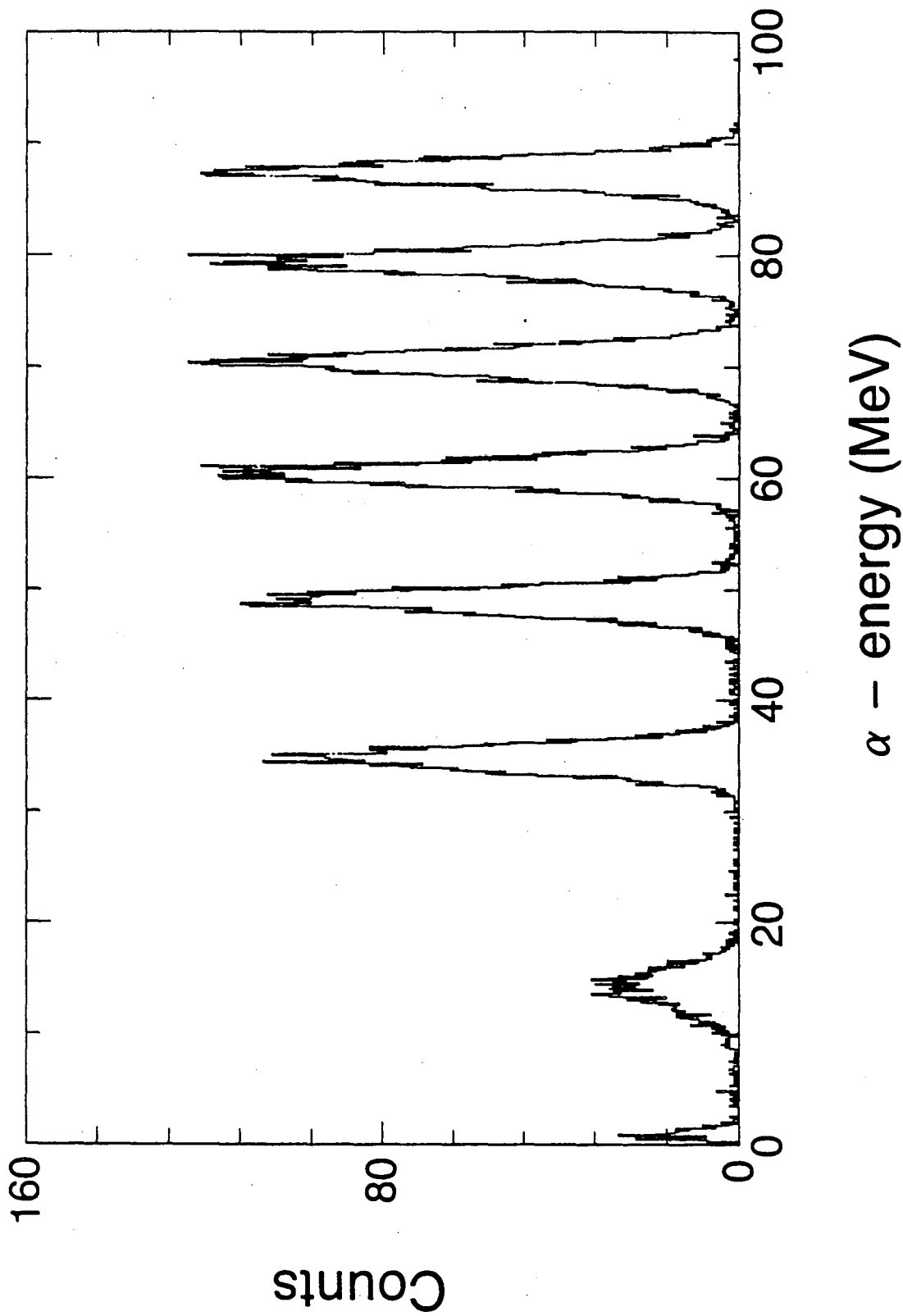
Fig. 2





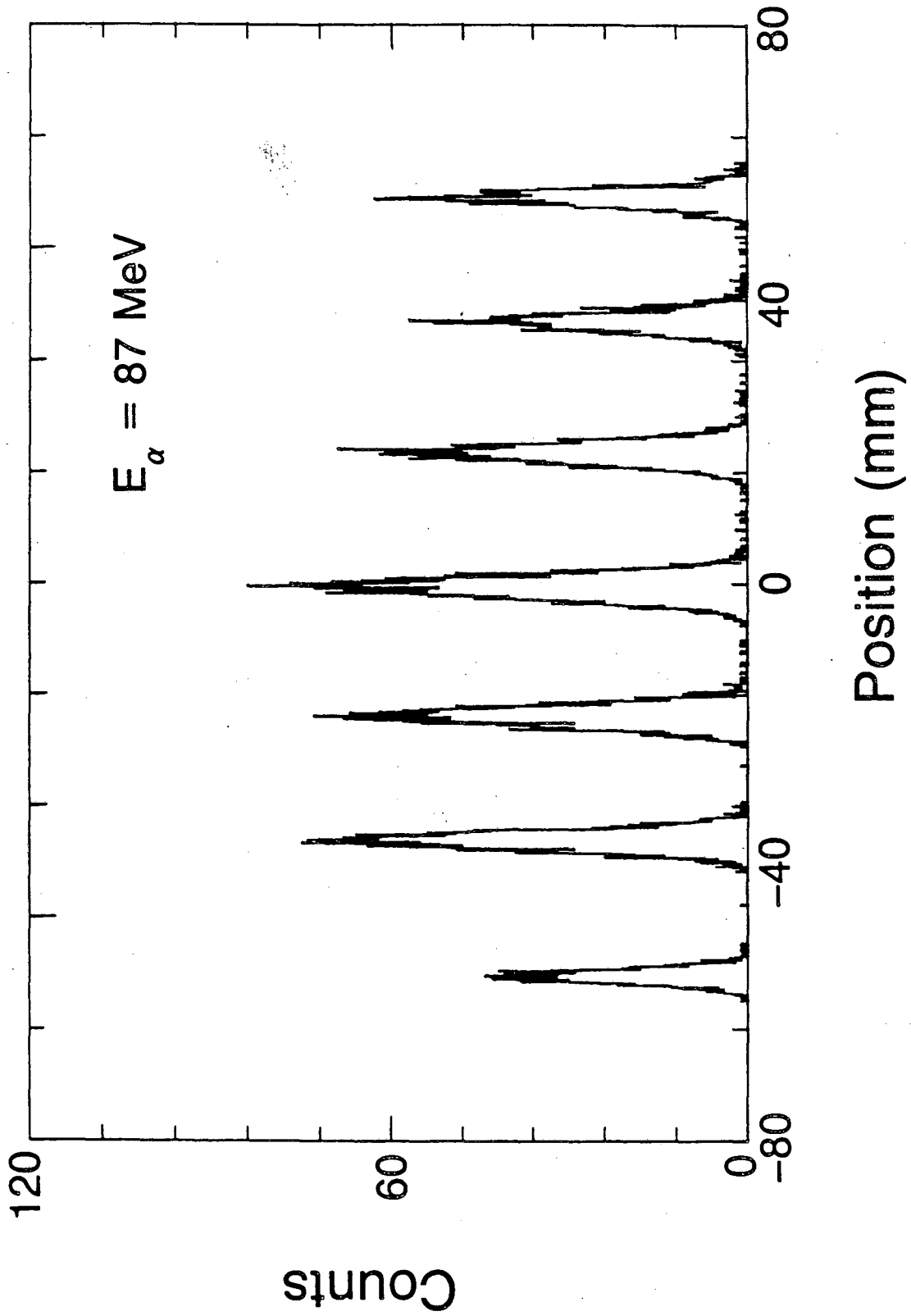
XBL 853-8047

Fig. 3



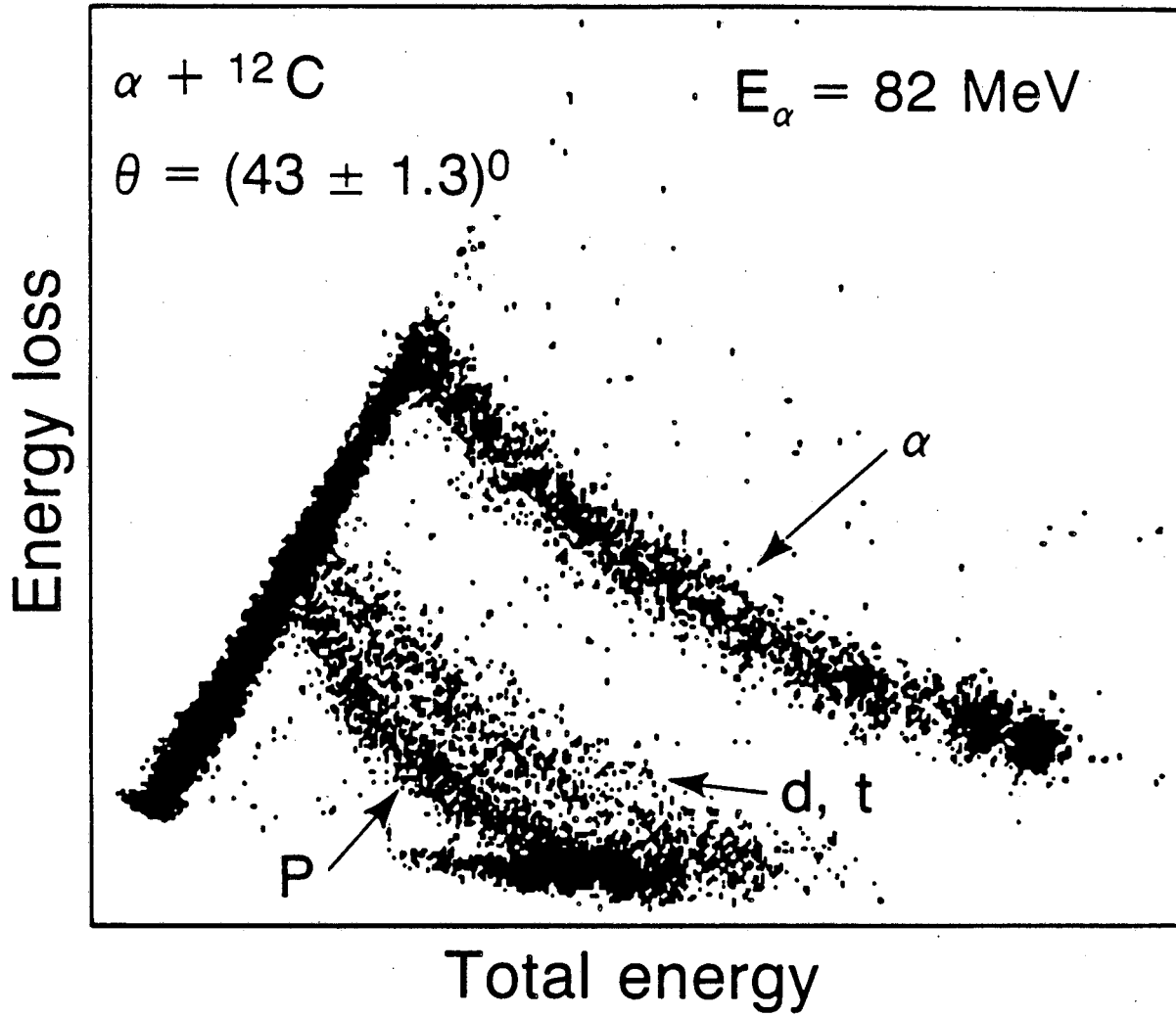
XBL 8411-6347

Fig. 4



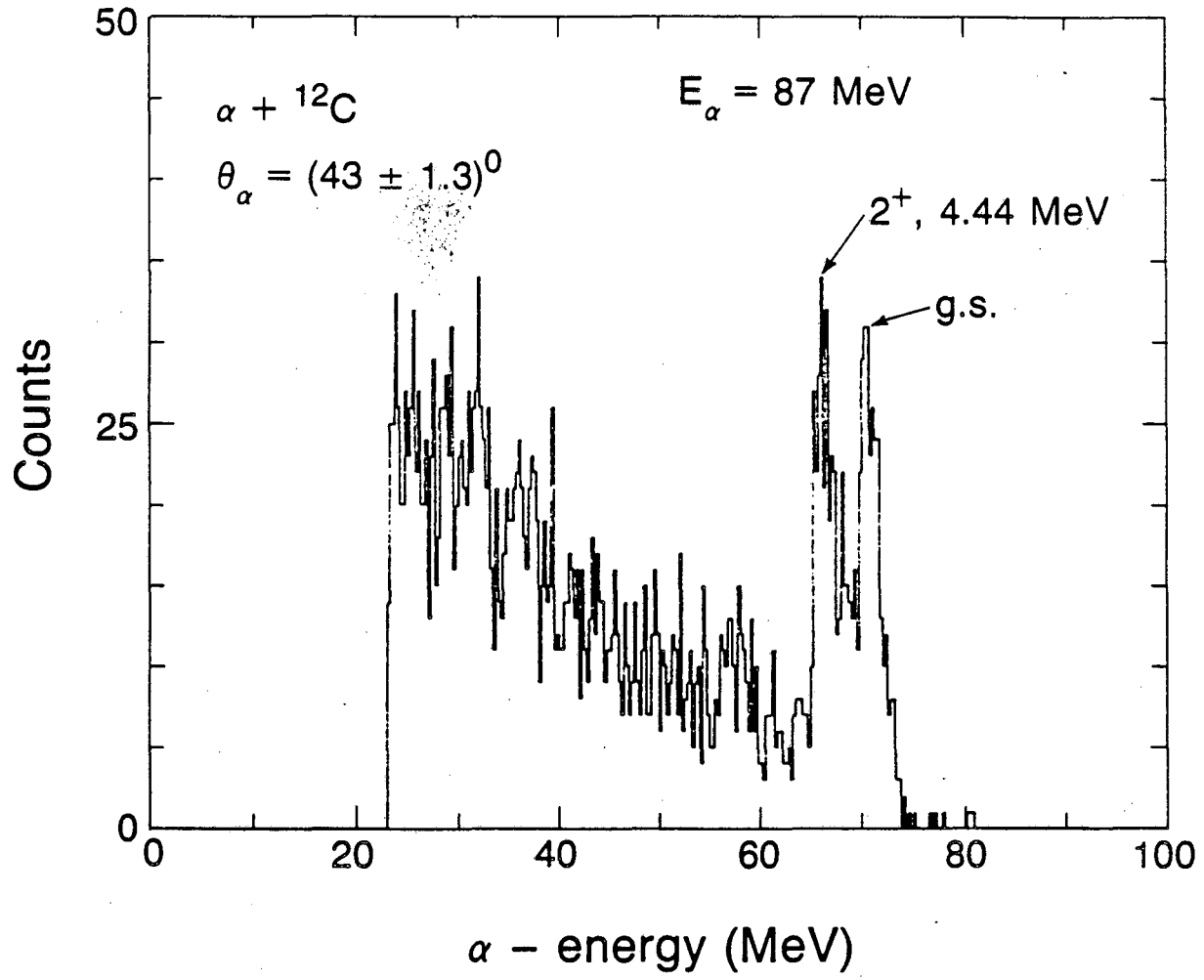
XBL 8411-6349

Fig. 5



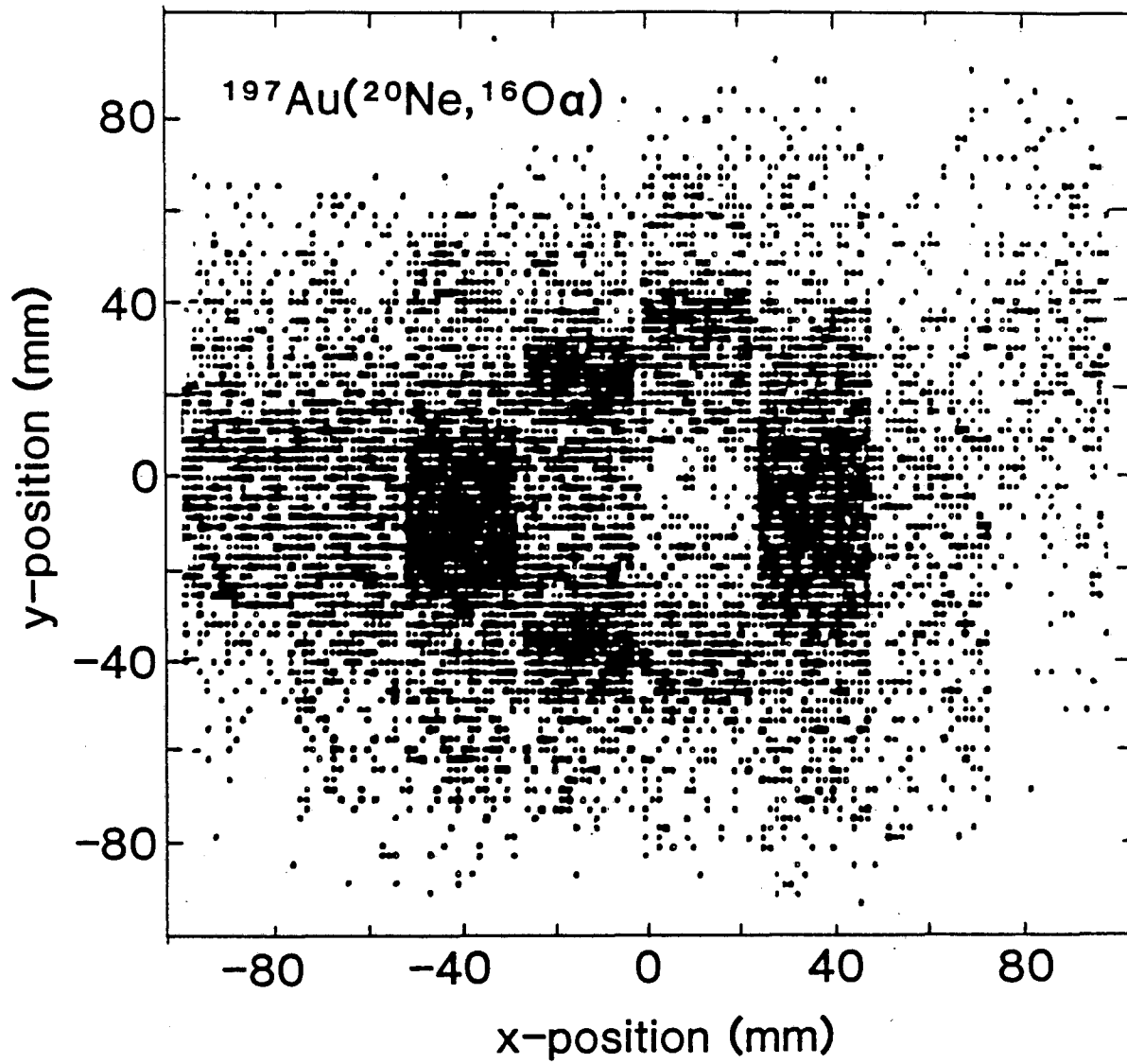
XBL 8411-6344

Fig. 6



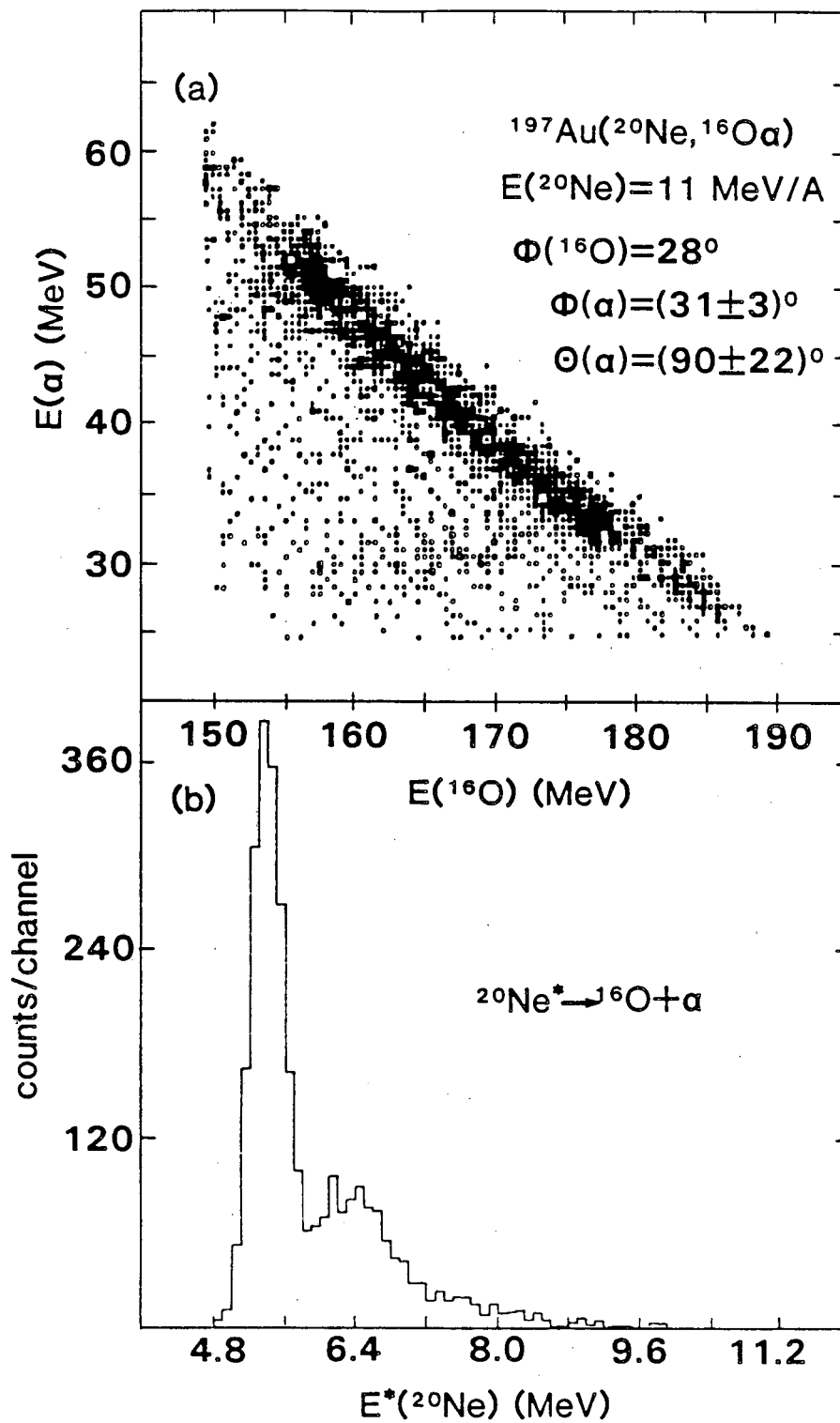
XBL 8411-6350

Fig. 7



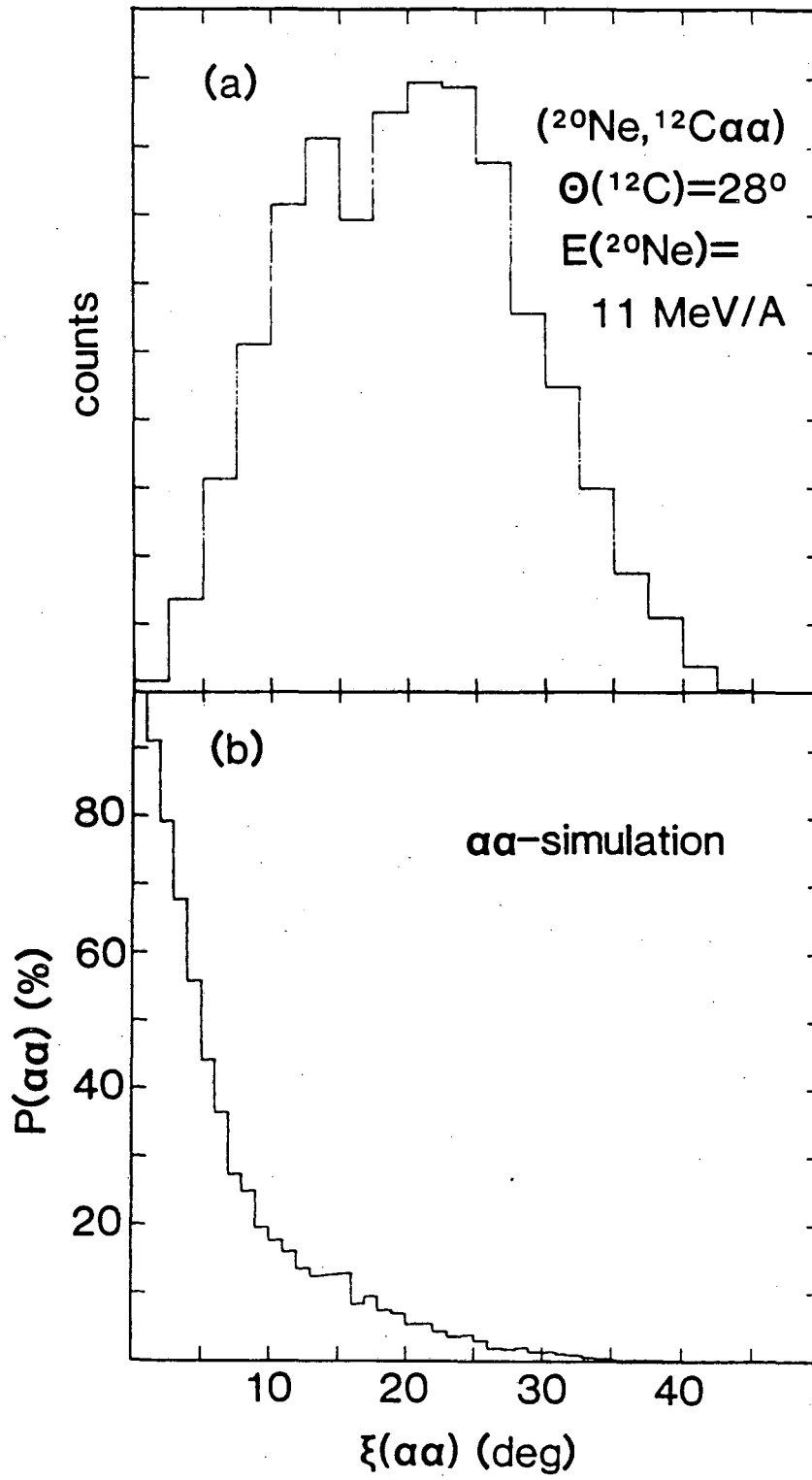
XBL 855-2329

Fig. 8



XBL 855-2330

Fig. 9



XBL 855-2331

Fig. 10



This report was done with support from the Department of Energy. Any conclusions or opinions expressed in this report represent solely those of the author(s) and not necessarily those of The Regents of the University of California, the Lawrence Berkeley Laboratory or the Department of Energy.

Reference to a company or product name does not imply approval or recommendation of the product by the University of California or the U.S. Department of Energy to the exclusion of others that may be suitable.

*LAWRENCE BERKELEY LABORATORY  
TECHNICAL INFORMATION DEPARTMENT  
UNIVERSITY OF CALIFORNIA  
BERKELEY, CALIFORNIA 94720*